HAMILTON, Robert Lee. THERMAL CONDUC-
TIVITY OF HETEROGENEOUS MIXTURES.

The University of Oklahoma, Ph.D., 1960
Engineering, chemical

THE UNIVERSITY OF OKLAHOMA

GRADUATE COLLEGE

THERMAL CONDUCTIVITY OF HETEROGENEOUS MIXTURES

A DISSERTATION

SUBMITTED TO THE GRADUATE FACULTY

in partial fulfillment of the requirements for the

degree of

DOCTOR OF PHILOSOPHY

BY

ROBERT LEE HAMILTON

Norman, Oklahoma

1960

THERMAL CONDUCTIVITY OF HETEROGENEOUS MIXTURES

APPROVED BY
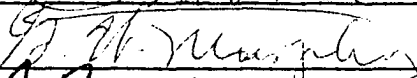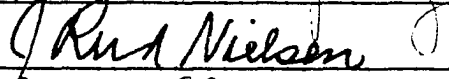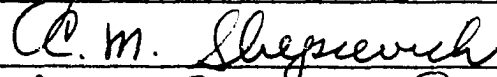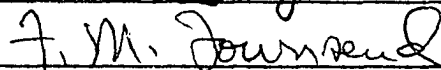
DISSERTATION COMMITTEE

ACKNOWLEDGMENT

TABLE OF CONTENTS

LIST OF TABLES

LIST OF ILLUSTRATIONS

THERMAL CONDUCTIVITY OF HETEROGENEOUS MIXTURES

CHAPTER I

INTRODUCTION

The purpose of this study was to find a general correlation for the thermal conductivity of a heterogeneous mixture as a function of the conductivity of its pure constituents. In order to do this, an experimental and theoretical investigation was made to determine those factors which influence the conductivity of a heterogeneous mixture. These factors included the properties of the pure constituents and the configuration and composition of the mixture.

Previous Theoretical Work

James Clerk Maxwell (10) was the first to work on the problem of conductivity of heterogeneous mixtures. He derived the equation:

$$\frac{(\frac{K}{K_1}) - 1}{(\frac{K}{K_1}) + 2} = V_2 \left[\frac{(\frac{K_2}{K_1}) - 1}{(\frac{K_2}{K_1}) + 2} \right] \qquad \text{I-1}$$

for the case of spherical particles of conductivity K_2 suspended in a continuous phase of conductivity K_1. In equation I-1, K is the conductivity of the mixture and V_2 is the volume fraction occupied by the spherical particles. The model used in deriving equation I-1 is shown

below, where the shaded portion of this sketch represents the continuous phase in Maxwell's model and the circles represent a cross section of the spherical particles. Notice that this equation gives the conductivity of the mixture in terms of the conductivities of the pure constituents and the volume fraction of the particles. This result does not include any reference to particle size. One may conclude, at least on a theoretical basis, that for a mixture of spheres suspended in a fluid the conductivity is not affected by the diameter of the spheres.
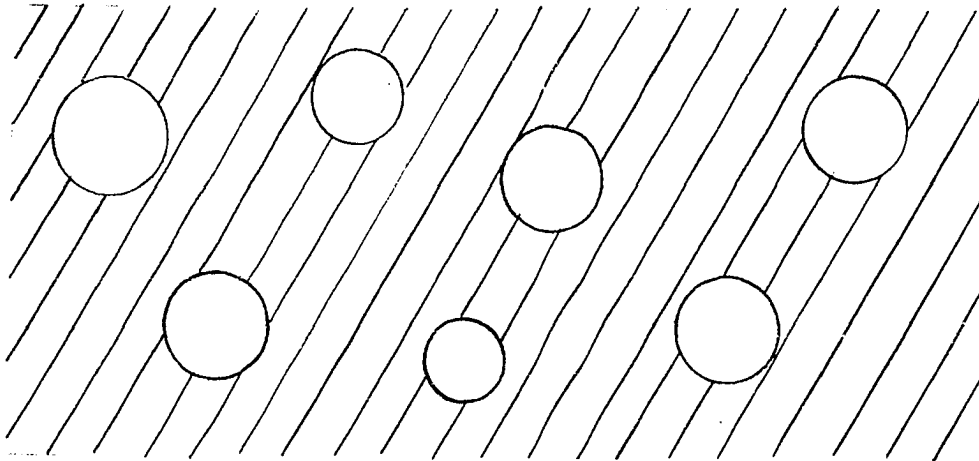
Figure I-1

In 1924, Fricke (5) extended Maxwell's analysis to the case of ellipsoids suspended in a continuous phase. His result is:

$$\frac{(\frac{K}{K_1}) - 1}{(\frac{K}{K_1}) + X} = V_2 \left[\frac{(\frac{K_2}{K_1}) - 1}{(\frac{K_2}{K_1}) + X} \right] \qquad \text{I-2}$$

where K, K_2 and K_1 are the conductivities of the mixture, particles

and continuous phase, respectively, and X is a complicated function of
the shape of the ellipsoids and, also, a function of K_1 and K_2. Fricke
concluded from his analysis that X, the "shape factor," is important
only if K_1 is much different from K_2. For the case where K_1 is ap-
proximately equal to K_2, X is approximately 2 and equation I-2 reduces
to I-1, independent of particle shape.

Physically, this conclusion means that the shape of the particles
forming the discontinuous phase is important only for the case where K_1
and K_2 differ greatly.

The previous theoretical work shows that for a mixture of spheri-
cal particles suspended in a continuous phase, the conductivity of the
mixture is independent of particle size; and that for a mixture of ellip-
soidal particles in a continuous phase the conductivity is a function of
the shape of the particle, particularly if the conductivities of the con-
stituents are widely different.

Previous Experimental Work

Extensive data have been published on systems such as porous
nickel, powdered copper, and porous graphite (4, 9, 6). These mixtures
consist of air pockets or inclusions interspersed in a continuous phase
of high conductivity material. The thermal conductivity of these mix-
tures decreases linearly with increasing volume fraction of air. This
relationship is indicated by the upper, straight line (curve I) in Figure
I-2.

An entirely different behavior is shown by mixtures such as metal-
lic particles suspended in a low conductivity material (7, 12). In this
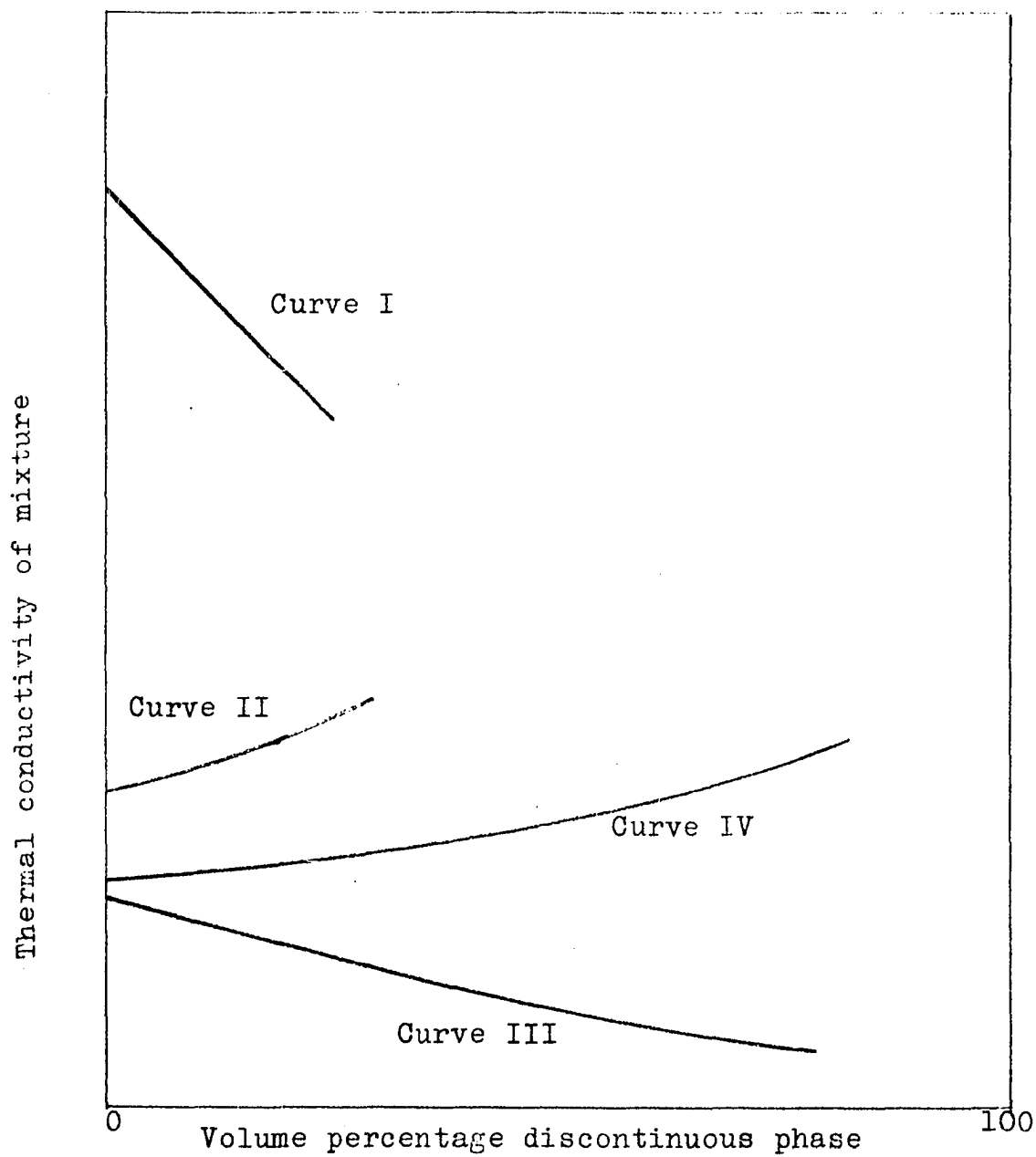
Figure I-2. General behavior of conductivity of heterogeneous mixtures

case the mixture conductivity increases <u>slightly</u> with increasing volume

fraction of metallic particles. This behavior is shown by curve II in

Figure I-2.

In the two types of mixtures discussed previously, the conductivi-

ties of the two constituents differed widely--by a factor of more than

one thousand. Two other types of mixtures are represented by curves III

and IV in Figure I-2. In these mixtures the conductivities are approxi-

mately equal. In one case (curve III), the continuous phase has a slightly

higher conductivity than the discontinuous phase; in the other, the con-

tinuous phase has a slightly lower conductivity (curve IV). Curves III

and IV might represent, for example, liquid-liquid emulsions (7, 14).

Figure I-2 represents the <u>data</u> on the conductivity of widely dif-

ferent types of mixtures, and indicates their diverse nature. This figure

also gives a basis for classifying mixtures. In the mixtures represented

by curves I and II, the conductivities of the pure constituents differ

widely. For example, in the case of porous copper containing air pockets

the conductivities differ by a factor of ten thousand. For the case of

metallic particles suspended in gelatine, the conductives differ by a

factor of one thousand. In such mixtures, the conductivity behavior de-

pends on whether the continuous phase has the higher or lower conductivity.

Mixtures having a high conductivity continuous phase and a low conductivi-

ty discontinuous phase are represented by curve I of Figure I-2 and will

be designated as <u>Class I</u>. Mixtures which have a low conductivity continu-

ous phase and a high conductivity discontinuous phase are represented by

curve II and will be designated as <u>Class II</u>. Mixtures in which the con-

stituents have approximately the same conductivity are represented by

curves III and IV and will be designated as <u>Class III</u> and <u>IV</u>, respec-
tively. In these two classes the conductivities of the constituents dif-
fer by less than a factor of one hundred. This classification is outlined
in Figure I-3, where specific examples are given for each class.

The data will now be discussed in detail. The object of this
discussion, which will be given by classes as outlined in Figure I-3,
will be to compare what is known experimentally about heterogeneous con-
ductivity with the conclusions drawn from available theory.

Marathe (9) has presented data on several Class I mixtures, in-
cluding compressed copper powder. For these mixtures, he found the con-
ductivity to be independent of particle size. (In this sense, the word,
"particle," refers to the air pockets or inclusions in the porous mater-
ials.) This observation agrees with the conclusions drawn from Maxwell's
work. Francl (4) gave the following empirical equation for the conduc-
tivity of Class I mixtures:

$$K = K_1(1 - V_2) \qquad\qquad I\text{-}3$$

where K is the conductivity of the porous metal; K_1 is the conducti-
vity of the pure metal; and V_2 is the volume fraction of air in the
porous metal. This equation indicates that the size and shape of the
discontinuous inclusions do not affect the conductivity of the porous
materials in Class I. Again, this result agrees with theory.

Data on Class II mixtures have been presented by Johnson (7). He
presented conductivities of mixtures of spherical copper particles sus-
pended in gelatin and on "drop-shaped" (sic) aluminum particles suspended
in gelatin.. The data on spherical copper particles in gelatin could be

High conductivity constituent is the continuous phase	Low conductivity constituent is the continuous phase
Class I $K_1 \gg K_2$ Phase '1' continuous. Foamed metals; porous metals; compressed metallic powders; ceramics	Class II $K_1 \ll K_2$ Phase '1' continuous. Suspensions of metallic particles in gelatin
Class III $1 < \dfrac{K_1}{K_2} < 100$ Phase '1' continuous. Liquid-liquid emulsions and suspensions	Class IV $1 < \dfrac{K_2}{K_1} < 100$ Phase '1' continuous. Liquid-liquid emulsions and suspensions; greases; suspensions of metallic oxides in gelatin

Figure I-3
Classification of heterogeneous mixtures

correlated with equation I-1, and it can be concluded that this equation correctly predicts the conductivity of such a mixture as a function of volume fraction of discontinuous phase (spheres).

The data on the mixture of "drop-shaped" aluminum particles in gelatin could not be correlated. The important feature of these data is the fact that for the same volume composition, the aluminum particles-gelatin mixture had a _higher_ conductivity than the mixture of copper spheres in gelatin. This result would seem unusual because the conductivity of aluminum is only about half that of copper. In view of Fricke's work, however, this anomoly could be explained as an effect of particle shape, which is the qualitative explanation offered by Johnson. In order to obtain a complete comparison between theory and experiment for these heterogeneous thermal conductivities, it may be concluded that additional experiments are necessary to determine the effect of particle shape for Class II mixtures. In this connection, de Vries (13) could find no data on the effect of particle shape in mixtures of this type. Furthermore, no data have been presented from which conclusions can be drawn concerning the effects of particle size and shape for mixtures of types Class III and Class IV.

The results of this review of previous experimental work can be summarized as follows: Class I mixtures can be correlated with equation I-3, and this equation implies that the conductivity of these mixtures is not a function of the shape or size of the inclusions which form the discontinuous phase. In Class II, both theoretical and experimental work indicate that there is an effect of particle _shape_. There was, however, only one experiment which applied, so that no quantitative conclusions

could be drawn. Theoretically, the size of the particles forming the Class II mixture does not affect the conductivity, but this had never been tested experimentally.

For Class III and Class IV mixtures, Fricke's (5) theoretical work indicates there is no effect of particle size or shape; but insufficient data could be found with which to test this conclusion.

CHAPTER II

EXPERIMENTAL

The literature review given in the last chapter left some questions unanswered. For example, according to Maxwell (10) the size of the particles forming the discontinuous phase does not affect the conductivity of the mixture. There is, however, no _experimental_ evidence for this conclusion.

Specifically, the questions to be answered by further experimental work are:

> What are the effects of particle size and shape in Class II mixtures?

> What are the effects of particle size and shape in Class III and Class IV mixtures?

> In all classes, what is the effect of volume fraction of the discontinuous phase?

Measurements were made on several mixtures of aluminum particles suspended in silicone rubber to determine the effects of particle size and shape in Class II mixtures. The mixtures varied in either particle size, or particle shape, or volume fraction of the discontinuous phase in such a way that the maximum information could be gained from each experiment. Aluminum was chosen for the discontinuous phase because it has a high conductivity and because it could be obtained as particles in a

variety of shapes, all of approximately the same purity. The rubber used

to suspend the particles could be vulcanized at room temperature with a

catalyst. This rubber was made by Dow-Corning Corporation (2) and is de-

signated "Silastic" (Dow-Corning trademark) RTV 502. This particular

rubber was used because its thermal conductivity had been measured (2).

A mixture of balsa wood particles in rubber was used to represent

Class III mixtures. Two different shapes of balsa particles were used:

One was disk shaped and the other was parallelepiped shaped.

In the early stages of the work, thermal conductivity measurements

were made on greases. These were chosen to represent Class IV mixtures

because they consist of soap particles interspersed in oil. The sizes

and shapes of these soap particles vary in different greases and thus

permit a determination of these effects.

Two types of conductivity cells were used in the measurements.

One was a spherical cell used for the Class II and Class III mixtures and

the other was a concentric cylinder cell used to measure the conductivity

of greases.

Apparatus and Procedure for Measuring the Conductivity
Of Class II and Class III Mixtures

Introduction. The measurements on Class II and III mixtures were

made with a steady-state, spherical cell. In this cell, heat was trans-

ferred through a spherical shell molded from the mixture. This spherical

shell surrounded a metal sphere which contained the heater resistance.

The temperature difference across the shell was about $5^{\circ}F$ and was measured

with thermocouples. With this cell configuration, the conductivity can

be calculated from the heat dissipated in the middle heater, the tempera-

ture difference across the spherical shell and the inside and outside diameter of the shell.

Experimental Apparatus. The cell was constructed by molding the mixture in the form of a spherical shell. The inside diameter of this shell was 1.50 inches. Two different outside diameters were used. One was 2.375 inches and the other was 3.5 inches. The inside heater consisted of a glass insulated 24-gage constantan wire imbedded in a sphere of solder. Figure II-1 shows a sketch of the cell and the heater and thermocouple wiring. Figure II-2 shows a photograph of the cell. The heater resistance was 0.40 ohms and the current in this resistor was measured by a General Electric, Type AP-11 A-C ammeter of a 0.25 per cent accuracy class. This current was regulated by a Powerstat (Superior Electric Co. trademark) and a Sola (Sola Electric Co.) A-C regulator. Copper-constantan thermocouples were used to measure temperatures. One junction of two of the thermocouples was imbedded in the solder which formed the heater. One junction of two other thermocouples was imbedded in the surface of the outside of the rubber mixture. The cold junctions of all thermocouples were kept at room temperature in a water bath. The voltages of these thermocouples were measured with a Leeds and Northrup Model 8662 potentiometer. With this potentiometer, a compensation could be made for the cold bath temperature, so that from the measured thermocouple voltage and a table of voltage versus temperature, the temperature of the thermocouple junction could be found.

Experimental Procedure. The mixture was prepared by stirring a weighed amount of particles into a measured volume of rubber and then adding 3 to 4 drops of the catalyst. This catalyst accelerated the vul-
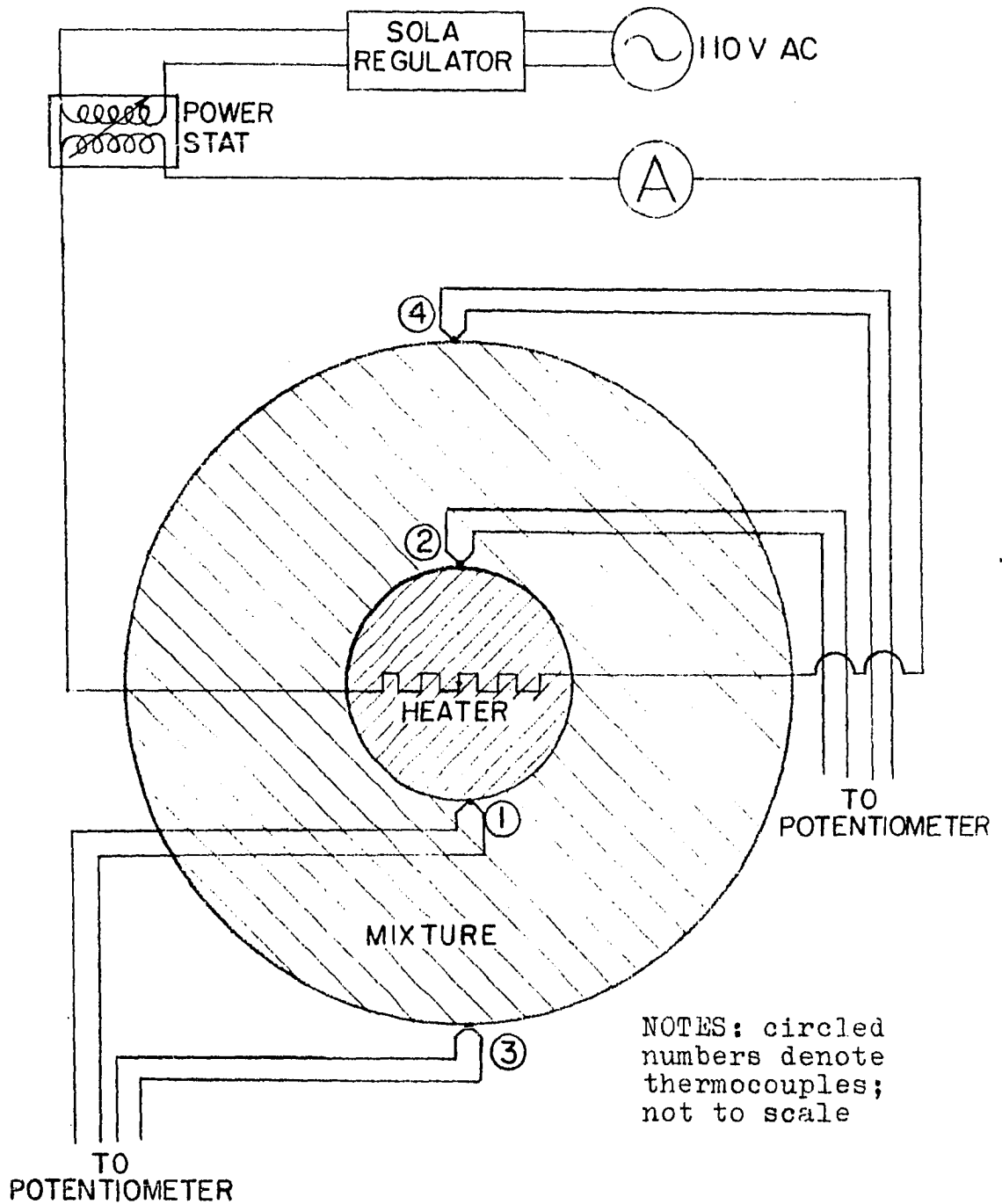
Figure II-1. Spherical conductivity cell
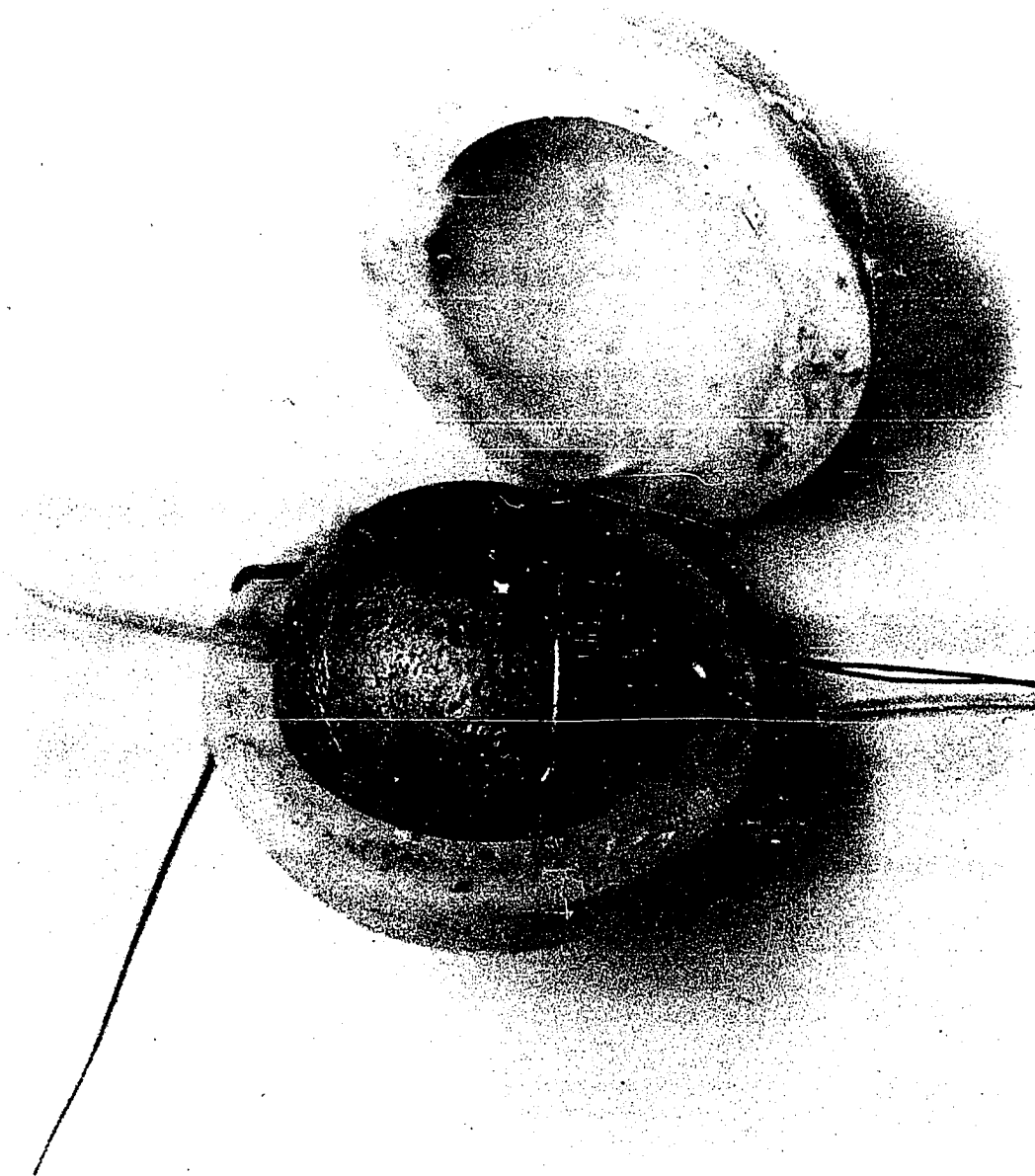
Figure II-2. Spherical cell

canization process. This catalyzed mixture was then poured into the mold. A celluloid sphere, 1.50 inches in diameter, formed the inside, and a hollow latex sphere formed the outside of the annulus mold. After the vulcanization was complete--usually about ten minutes--the outside mold was removed and the shell was cut along a great circle and the celluloid sphere was removed so the heater could be put inside the shell. A small amount of freshly catalyzed rubber was spread over the surface of the heater to be sure the heater surface was in good thermal contact with the inner surface of the shell. After enclosing the heater in the shell, two thermocouple junctions were imbedded in the outer surface of the shell. The cell was then suspended inside a large enclosure and the heater was turned on. After one or two hours the inside and outside thermocouple voltages and the current in the heater were recorded. The data and sample calculations are given in the appendix.

Preliminary Measurement and Experiments. The resistance of the heater, used in calculating the heater power, was measured in a bridge circuit in which it was compared with a standard 1.00 ohm resistor. The resistance of the heater was 0.40 ohms. The first conductivity measurements were made on the pure rubber. These measured values are given in Table II-1 where they are compared with the value given by the manufacturer. In this set of measurements, two shells of different outside diameters were used to insure that the measured conductivities did not depend on the cell size.

During these preliminary measurements, the outside thermocouple junctions were moved from place to place around the outside surface of the spherical shell. This measurement showed that the outside tempera-

ture varied by only 0.1°F over the outer surface of the shell.

TABLE II-1

COMPARISON OF MEASURED CONDUCTIVITY OF RUBBER WITH
THE VALUE GIVEN BY THE MANUFACTURER (2)

Cell Dimensions		Measured Conductivity $Btu/ft^2/hr\text{-}°F/ft.$	Manufacturer's Value $Btu/ft^2\text{-}hr\text{-}°F/ft.$
Inside Diameter (Inches)	Outside Diameter (inches)		
1.50	2.375	0.125	0.127
1.50	3.500	0.130	0.127

To check the uniformity of the mixtures, X-rays were taken of a sample of the mixtures used in the measurements. Figure II-3 shows X-ray pictures of two mixtures of aluminum spheres in rubber. These photographs represent slices, 1/8 inch thick, cut from hemispheres of the mixtures. One mixture contained 15 volume per cent and the other 30 volume per cent spherical aluminum particles.

Figure II-3. X-ray of spherical aluminum particles-rubber mixtures. Top picture-15 volume per cent. aluminum; Bottom picture-30 volume per cent. aluminum. Both samples were approximately 1/8 inch thick.

Apparatus and Procedure for Measuring the
Conductivity of Greases

Experimental Apparatus. The apparatus was a guarded, steady-state, concentric cylinder cell. It consisted of a central bar containing three independent heater sections: a middle heater and two guard heaters. This central bar was surrounded by an aluminum tube (11.260 inches long and 1.650 inches I. D. and 1.868 inches O. D.) so as to leave an annular space (1.496 inches I. D. by 1.650 inches O. D.) for the sample. The outer aluminum tube and the central bar were aligned concentrically by means of Teflon (Du Pont trademark) spacers (Figure II-6) at each end of the cell. The disassembled cell is shown in Figure II-4 and the details of the design are shown in the drawing of Figure II-8.

The middle heater and the two guard heaters were each constructed by cutting a 0.060 inches wide and 0.055 inches deep rectangular spiral groove, six turns per inch, in a hollow aluminum bar and winding a 24-gauge, glass insulated, "constantan" wire into the spiral groove. A tight-fitting aluminum sleeve (1.4975 inches O. D.) was slipped over the heater wires. These sleeves were in contact with both the heater wire insulation and the aluminum bar. The copper heater leads were joined to the constantan heater wires at the ends of the spiral grooves and were led out of the heater section through a small slanting hole cut into each end of the heater. The copper leads were led from this slanting hole into a 3/8 inch diameter axial hole extending through the center section and out of the top of the cell. The two assembled guard heater sections were then connected to the assembled middle heater section with Teflon plugs. These plugs were of the same diameter as the aluminum heater sleeves.
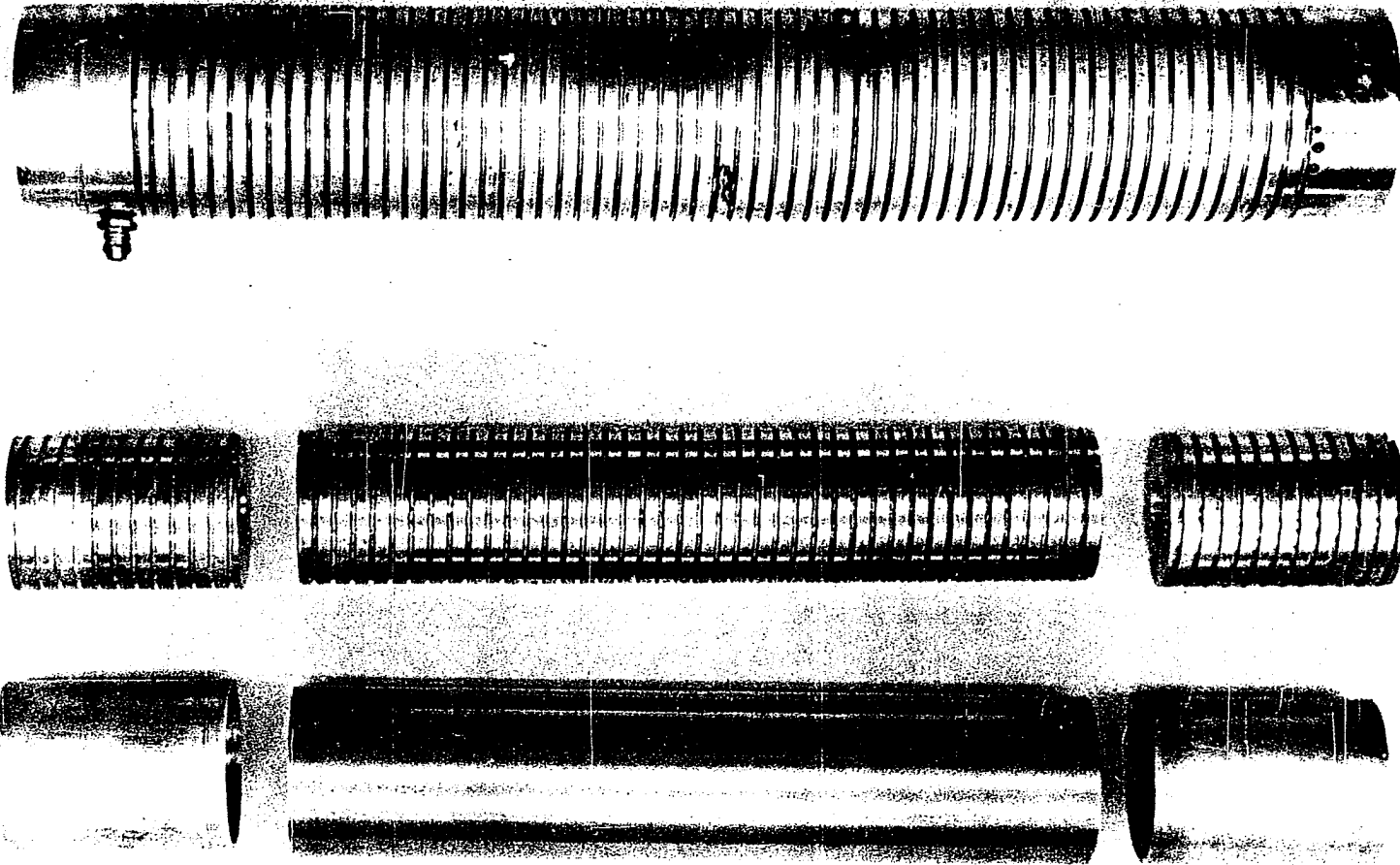
Figure II-4. Disassembled cylindrical cell
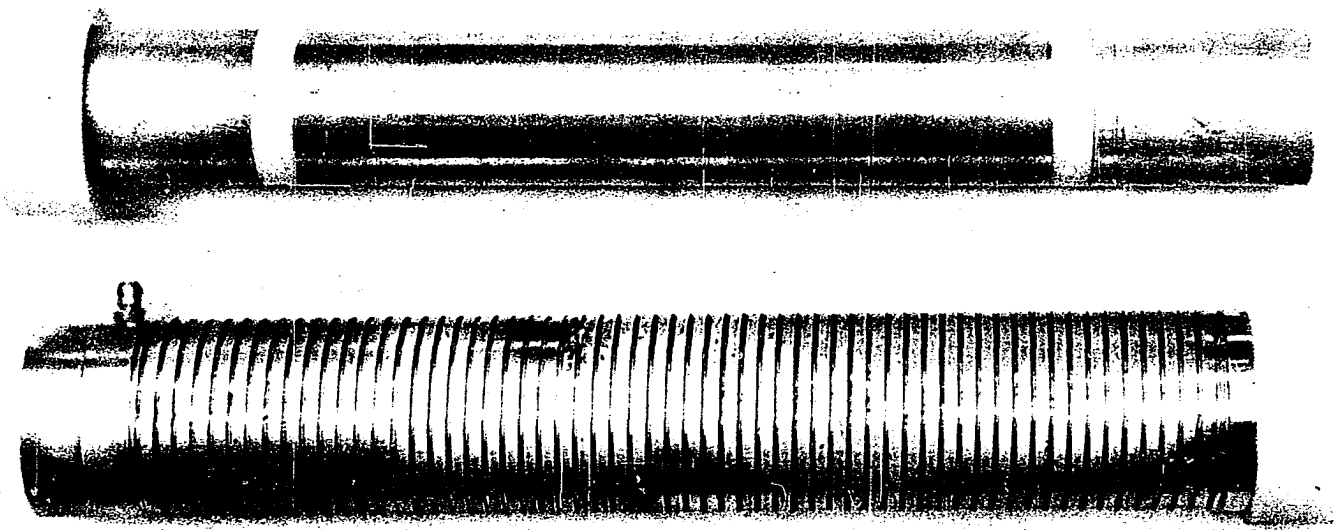
Figure II-5. Assembled central bar and outer tube
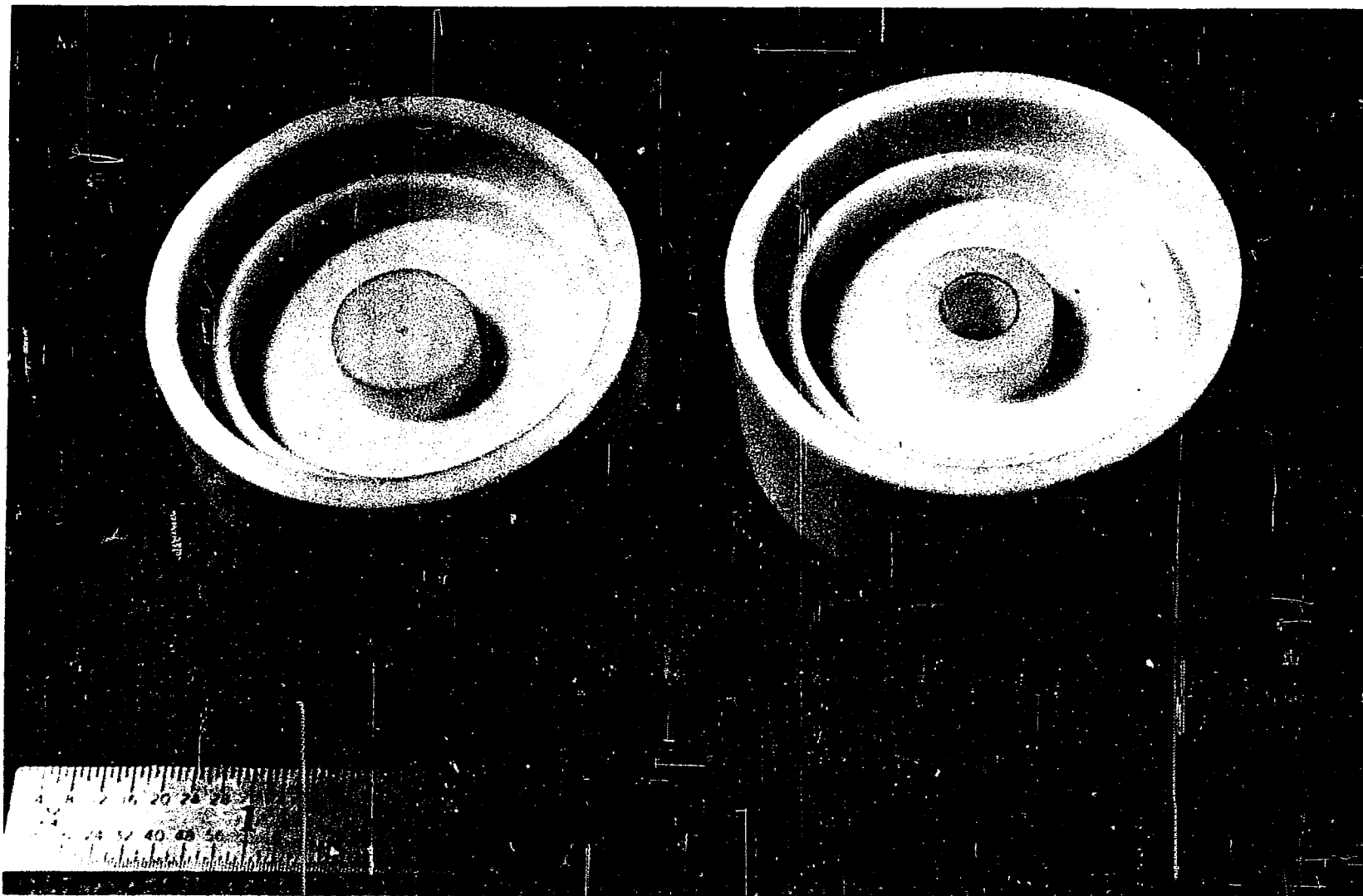
Figure II-6. End spacers

Figure II-7. Teflon plugs

TEFLON SPACER OUTSIDE TUBE 1.6500"I.D. ANNULUS GREASE GUN FITTING

1/8" HOLE

HEATER WIRE MIDDLE HEATER TEFLON PLUG

3/8 HOLE

TOP GUARD SLEEVE 1.4975" O.D. HEATER LEAD WIRE

1/8 HOLE

2.1"

6.885"

L = 7.260"

2.1"
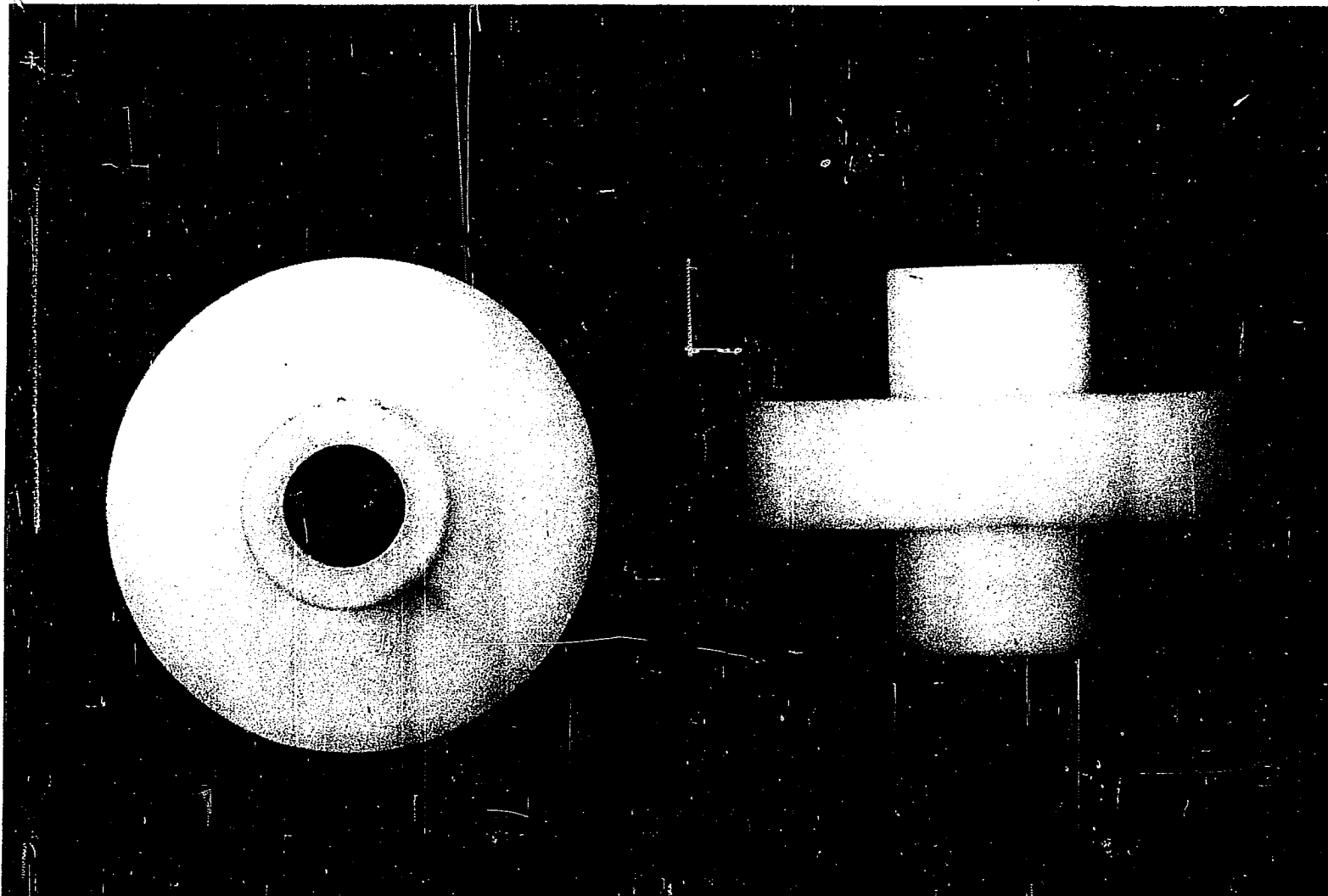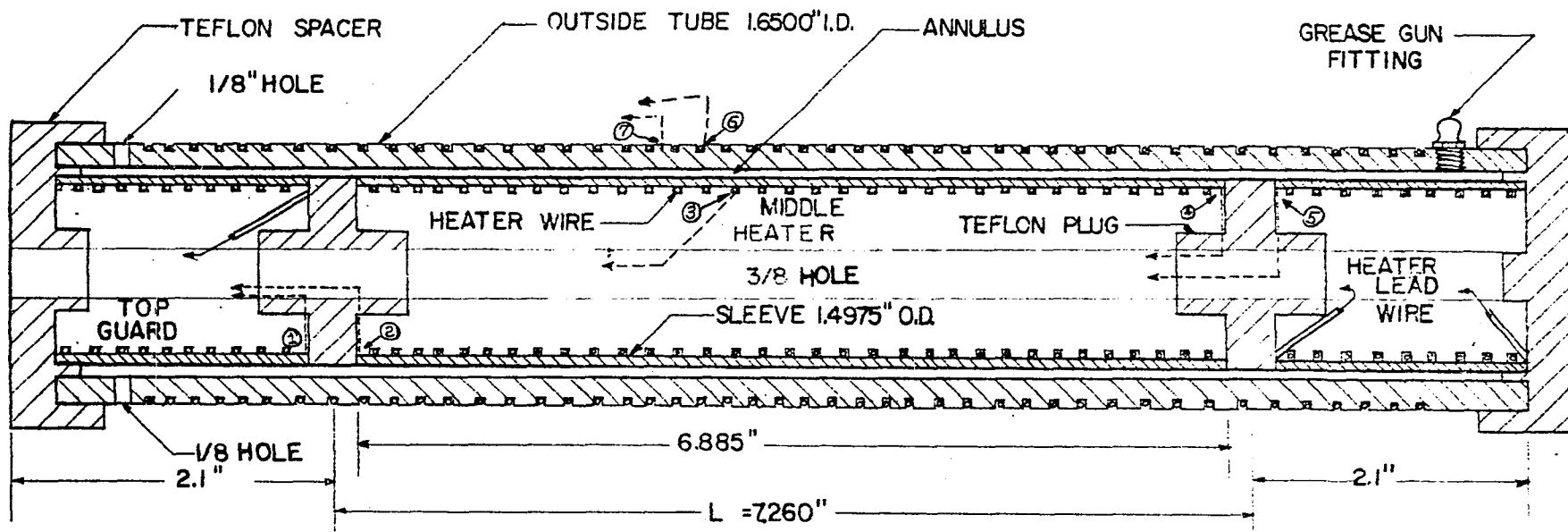
NOTES: circled numbers
denote thermocouples;
scale--approximately
3/4 full size

Figure II-8. Cylindrical conductivity cell

Figure II-5 shows the assembled center bar and the outer tube.

A 30-gauge copper-constantan thermocouple junction was located on either side of each Teflon plug between the plug and the aluminum sleeve. The positions of these thermocouple junctions are shown in Figure II-8. The thermocouple leads were led through a small radial hole (shown as dotted lines in Figure II-8) into the 3/8-inch axial hole and then out of the top of the cell. The cold junctions of these thermocouples were insulated with Teflon tubing and placed in holes drilled in a one inch diameter by four inch long copper bar. This copper bar was placed in a one gallon vessel of water which was kept at room temperature. Thermocouple voltage measurements were made with a Leeds and Northrup Model 7552 potentiometer.

The outside tube was made by cutting a 0.06 inch wide by 0.04 inch deep rectangular, spiral groove, six turns per inch, on the outside of an aluminum tube. A glass insulated chromel heater wire was wound into this groove. Two thermocouple junctions were soldered with tin into holes drilled into the outside tube. One of the thermocouple holes was located under the heater wire; the other was located between two successive turns of heater wire, as shown in Figure II-8. The cold junctions of these two thermocouples were placed in the previously described water bath. A grease gun fitting was located near the bottom of the outside tube; also, two 1/8-inch holes, diametrically opposite each other, were drilled into the outside tube near the top of the cell.

After the central bar was assembled, it was placed inside the outside tube and was aligned using the accurately machined Teflon spacers at each end. Figure II-6 shows these two spacers; the one on the right

was used at the top of the cell and the lead wires were led out of the central hole. The thickness of the thin, inner rim of these spacers was that of the annular space in the cell.

The outside heater and the two guard heaters used alternating current. The middle heater used direct current supplied from a continuously charged six volt battery. Direct current was used in the middle heater so that this current could be measured accurately ($\pm$ 0.2 per cent) with the Leeds and Northrup 7552 potentiometer. This measurement was made by placing a standard 0.001 ohm resistor in series with the middle heater and measuring the voltage drop across this resistor. The resistance of the middle heater, which was also needed to calculate the power dissipated in the middle heater section, was 4.410 ohms.

Preliminary Measurements. After the cell was assembled, several tests were necessary before the measurements on grease could be carried out. The resistance of the middle heater was measured using a bridge type circuit that permitted comparison of the middle heater resistance with a standard 10.000 ohm resistor. The middle heater resistance was found to be 4.410 $\pm$ 0.007. This value was the average of six measurements; it was also checked at higher temperatures and it was found to be the same.

Effect of Axial Heat Loss. In designing the cell, it was assumed that there would be no axial temperature difference across the Teflon plugs. It was not feasible, however, to meet this condition in the experiments. So, the effect of an axial temperature difference across the Teflon plugs had to be calculated. These calculations are given in the appendix. If the temperature difference across one of the Teflon plugs were 0.5°F and if the middle heater current were 1 amp, then the heat

loss across a Teflon plug would be only 0.4 per cent of the heat generated in the middle heater. Thus, a temperature difference as large as 0.5 ^{o}F across these plugs would not affect the value of thermal conductivity.

Sample Loading. In order to be sure the grease sample would fill the annular space if loaded with the grease gun, a full size glass replica of the cell was constructed. This model had an annular space essentially the same size as the cell. Grease was pumped into this model and the annular space was completely filled. No air spaces were present in the center section.

Free Convection in Oil Samples. The grease oil was placed in the annulus of the model and heated at the inside of the annulus. With a temperature difference across the annulus of approximately 20°F there was no apparent convection after 4 to 5 hours. Presumably, even if some laminar convection existed, it would not affect the measured thermal conductivity.

Experimental Procedure and Calculations. The test material was placed in the cell. Liquids were introduced through the two holes in the top of the outside tube by means of a hypodermic syringe. Greases were pumped into the annulus through the grease gun fitting at the bottom of the cell (see Figure II-8). The inside heaters--the middle heater and both guard heaters--were turned on. The outside heater powerstat was set to give the desired average temperature. After two to three hours, the guard heaters were adjusted so that there would be very little temperature difference across either Teflon plug. Additional guard heater adjustments were made as necessary. After another two or three hours, the temperature differences across the Teflon plugs would be about 0.1 to

0.5°F and the average cell temperature would be constant. When thermo-
couple voltages and voltage drop across the standard resistances were con-
stant for a period of two hours, the data established a thermal conducti-
vity (see Appendix for sample calculations). The average temperature of
the sample was taken as the arithmetic average of the inside and the out-
side temperatures.

Measurements on Glycerine. At this point, measurements were made
on glycerine whose thermal conductivity had been measured by other (15)
apparatus. Glycerine has about the same values for thermal conductivity
and viscosity as oils. Table II-2 compares the results for glycerine of
Woolf and Sibbitt (15) with that measured with this apparatus. These
tables show that the apparatus gave reasonably accurate and reproducible
values for thermal conductivity.

TABLE II-2

COMPARISON OF DATA FOR GLYCERINE WITH RESULTS OF
WOOLF AND SIBBITT

Temperature °F	Woolf and Sibbitt	This Work	Annular Temperature Difference °F	Per Cent Difference
137	0.161	0.154	8	4.3
154	0.162	0.154	10	4.4
160	0.162	0.156	10	4.3

These tables also show that the measured value of K is not a
strong function of temperature difference across the annulus. The repro-

ducibility, however, is a function of this temperature difference. This result is understandable because this temperature difference can be measured only to $\pm 0.1^{\circ}F$. If the difference is $1.0^{\circ}F$, the reproducibility is $\frac{0.1}{1.0}$ x 100 = 10 per cent, and if the difference is $10^{\circ}F$, the reproducibility would be $\frac{0.1}{10}$ x 100 = one per cent. The precision of the measurements of the current to the center heater improves as the temperature difference across the annulus increases for the same reason. The reproducibility of the apparatus was determined experimentally by taking several measurements at different values of annulus temperature difference. The reproducibility is defined as the maximum difference between any two measurements of thermal conductivity divided by their arithmetic average. These measurements showed that the deviation decreased almost linearly with temperature difference. At a temperature difference of 7 to $10^{\circ}F$, which was used in the grease measurements, the reproducibility was about 2 to 3 per cent.

CHAPTER III

THEORETICAL

In this chapter an equation will be derived which will correlate all the data presented in the previous chapters. The physical model used will assume that the composite media is made up of particles of conductivity, K_2, suspended in an otherwise continuous phase of conductivity, K_1. Figure III-1 shows a slab of this composite media. A set of rectangular coordinates is constructed as shown in the drawing. The thickness of the slab is "L" in the X-direction, and the slab is considered to have unit dimensions in the Y and Z-directions.
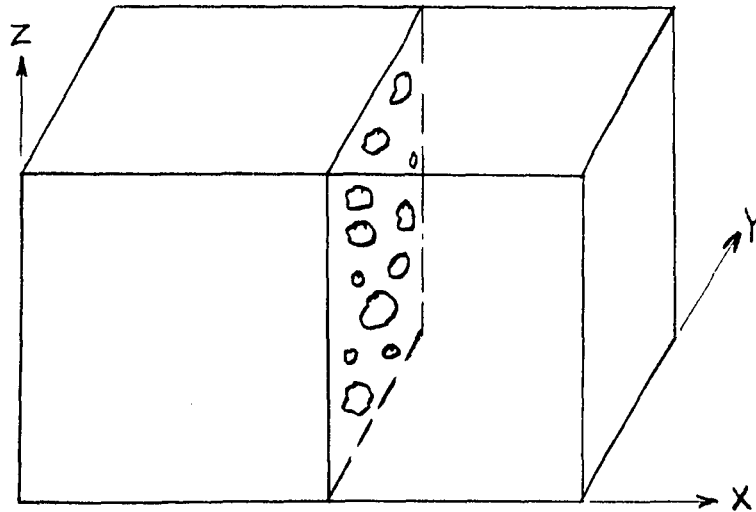
Figure III-1. Physical model for derivation of equation.

A plane, perpendicular to the X-direction, is passed through the slab of the composite medium. This plane intersects various individual particles and the total area of the plane intersected by the particles (Phase 2) will be called A_2. Heat is flowing through the slab in the X-direction only.

The heat flowing through A_2 is:

$$Q_2 = K_2 A_2 \left(\frac{dT}{dx}\right)_2 , \qquad\qquad III\text{-}1$$

where Q_2 is the heat flowing through the area representing the intersection of the particles with the plane; K_2 is the conductivity of the particles; A_2 is the area representing the intersection of the particles with the plane; and $(dT/dx)_2$ is the temperature gradient in the particles at the plane. The heat flowing through the continuous phase at the plane will be:

$$Q_1 = K_1 A_1 \left(\frac{dT}{dx}\right)_1 , \qquad\qquad III\text{-}2$$

where Q_1 is the heat flowing through the continuous phase at the plane; K_1 is the conductivity of the continuous constituent; A_1 is the area representing the intersection of the continuous phase with the plane; and $(dT/dx)_1$ is the temperature gradient in the continuous phase.

The total amount of heat crossing the plane will be the sum of the heat crossing the plane through the particles and the heat crossing the plane through the continuous phase. This total is:

$$Q_{plane} = Q_1 + Q_2 = K_1 A_1 \left(\frac{dT}{dx}\right)_1 + K_2 A_2 \left(\frac{dT}{dx}\right)_2 . \qquad III\text{-}3$$

Or,

$$Q_{plane} = \sum_{1,2} Q_i = \sum_{1,2} (KA \frac{dT}{dx})_i . \qquad \text{III-4}$$

The total heat flow through the slab is:

$$Q_{slab} = K A_{slab} (\frac{\Delta T}{L})_{slab} , \qquad \text{III-5}$$

where K is the conductivity of the mixture; A_{slab} is the area of the slab and $(\Delta T/L)$ is the temperature difference across the slab (in the X-direction) divided by the thickness of the slab, L. Notice equation III-5 is simply the operational definition of the conductivity of the mixture. It is the equation by which K would be measured in the laboratory, and K is the quantity which is to be predicted.

At steady-state, the heat flowing through the slab also passes through the plane; or:

$$Q_{slab} = Q_{plane} .$$

Or, from equations III-4 and III-5:

$$K A_{slab} (\frac{\Delta T}{L})_{slab} = \sum_{1,2} (KA \frac{dT}{dx})_i . \qquad \text{III-6}$$

Solving equation III-6 for K gives:

$$K = \sum_{1,2} K_i (\frac{A_i}{A_{slab}}) \frac{(\frac{dT}{dx})_i}{(\frac{\Delta T}{L})_{slab}} . \qquad \text{III-7}$$

If equation III-7 is to be perfectly general, A_{slab} and $(\Delta T/L)_{slab}$ must be eliminated by other equations, because K should not depend on the geometry of the slab. A_{slab} can be eliminated by assuming:

$$A_i/A_{slab} = V_i , \qquad\qquad \text{III-8}$$

where V_i is the volume fraction of the ith component. This equation says that the fraction of the plane intersected by the particles is proportional to the volume fraction of particles, which does not seem to be an unreasonable assumption.

An expression for $(\Delta T/L)_{slab}$ can be found as follows: Construct a line in the X-direction through the slab. Let L_1 represent the total length of this line lying in the continuous phase; and let L_2 represent the total length of this line lying in the discontinuous phase. If the temperature differences are added along this line, their sum must equal the temperature difference across the slab. In symbols:

$$(\Delta T)_1 + (\Delta T)_2 = (\Delta T)_{slab} \qquad\qquad \text{III-9}$$

$$\text{Also,} (\Delta T)_1 = \left(\overline{\frac{dT}{dx}}\right)_1 L_1 \quad \text{and} \quad (\Delta T)_2 = \left(\overline{\frac{dT}{dx}}\right)_2 L_2 \qquad \text{III-10}$$

where the "superbars" infer that the gradients are _averaged_ over the phases.

Certainly: $(\Delta T)_{slab} = \left(\frac{\Delta T}{L}\right)_{slab} L_{slab}$ \qquad\qquad III-11

Combining the last three equations gives:

$$\left(\overline{\frac{dT}{dx}}\right)_1 L_1 + \left(\overline{\frac{dT}{dx}}\right)_2 L_2 = \left(\frac{\Delta T}{L}\right)_{slab} L_{slab} \qquad \text{III-12}$$

$$\text{or,} \quad \sum_{1,2} \left\{ \left(\overline{\frac{dT}{dx}}\right)_i \frac{L_i}{L_{slab}} \right\} = \left(\frac{\Delta T}{L}\right)_{slab} \qquad \text{III-13}$$

The same statements apply to L_i/L_{slab} as were made earlier concerning $A_i/A_{slab} = V_i$, so that it is assumed that $L_i/L_{slab} = V_i$ Equation

III-13 can now be written:

$$\left(\frac{\Delta T}{L}\right)_{slab} = \sum \left(\frac{dT}{dx}\right)_i V_i \quad . \qquad\qquad \text{III-14}$$

If it is assumed that $(dt/dx)_i$ in III - 14 can be identified with $(dt/dx)_i$

in III - 7, these two equations can be combined to give:

$$K = \frac{\sum_{1,2} K_i V_i \left(\frac{dT}{dx}\right)_i}{\sum_{1,2} V_i \left(\frac{dT}{dx}\right)_i} \quad . \qquad\qquad \text{III-15}$$

This equation might be considered nothing more than an averaging equation

for thermal conductivity. K can be considered a summated average rather

than an integrated average.

It will be worthwhile to examine some of the features of equation

III-15. If, for example, it is assumed:

$$\left(\frac{dT}{dx}\right)_1 = \left(\frac{dT}{dx}\right)_2 \quad , \qquad\qquad \text{III-16}$$

equation III-15 becomes:

$$K = \frac{\sum K_i V_i}{\sum V_i} \quad . \qquad\qquad \text{III-17}$$

Since $\sum V_i = 1$, equation III-17 becomes:

$$K = \sum K_i V_i \quad . \qquad\qquad \text{III-18}$$

This is the equation for resistances in parallel arrangement. On the

other hand, if we let:

$$\left(\frac{dT}{dx}\right)_i \propto \frac{1}{K_i} \quad , \qquad\qquad \text{III-19}$$

equation III-15 becomes:

$$K = \frac{1}{\sum \frac{V_i}{K_i}} \; , \qquad\qquad \text{III-20}$$

which is the equation for resistances arranged in _series_.

Since this study deals with _binary_ mixtures in which one phase is continuous and the other is discontinuous, the summations in equation III-15 will be over components "1" and "2." The continuous phase will be designated phase "1," and the discontinuous phase will be designated phase "2."

For this discussion of binary mixtures it will be convenient to discuss the ratio of the average temperature gradients in the two phases, instead of considering them independently. When both denominator and numerator of equation III-15 are divided by $(dT/dx)_1$, the temperature gradient in the continuous phase, the result is:

$$K = \frac{\displaystyle\sum_{1,2} K_i \, V_i \, \frac{\left(\frac{dT}{dx}\right)_i}{\left(\frac{dT}{dx}\right)_1}}{\displaystyle\sum_{1,2} V_i \, \frac{\left(\frac{dT}{dx}\right)_i}{\left(\frac{dT}{dx}\right)_1}} \; . \qquad\qquad \text{III-21}$$

This analysis of the problem indicates that the effects of composition and conductivities of constituents can be accounted for by a weighted average of conductivities. The weighting factor is the product of volume fraction and temperature gradient ratio. This gradient ratio must be, in its most general context, a function of the discontinuous phase particle shape and arrangement and the thermal conductivities.

For _spheres_, suspended in an otherwise continuous medium, Maxwell (10) gives the relation:

$$\frac{\left(\frac{dT}{dx}\right)_i}{\left(\frac{dT}{dx}\right)_1} = \frac{3K_1}{K_i + 2K_1} . \qquad \text{III-22}$$

Substituting III-22 into III-21 gives for a binary mixture:

$$K = \frac{K_1 \left[K_2 + 2K_1 - 2V_2(K_1 - K_2)\right]}{K_2 + 2K_1 + V_2(K_1 - K_2)} , \qquad \text{III-23}$$

where K is the conductivity of the mixture; K_1 is the conductivity of the constituent forming the continuous phase; K_2 is the conductivity of the constituent forming the discontinuous phase; and V_2 is the volume fraction of discontinuous phase.

Equation III-23 will correlate the data on mixtures consisting of spherical particles suspended in an otherwise continuous medium. For example, III-23 checks well with the data on spherical copper particles suspended in water (7), liquid-liquid emulsions (14), and other mixtures of this type. Equation III-23 agrees neither with the data on cylindrical aluminum particles in water nor with the data (12) on graphite discs suspended in oil. This failure of equation III-23 is evidently due to the shape of the aluminum and graphite particles: Neither were spherical. This failure is not surprising in view of the fact that equation III-22, which was derived specifically for spheres, was used in deriving equation III-23. In order to account for these effects of particle shape, which are significant for class II mixtures, it is proposed to change equation III-22 to:

$$\frac{\left(\frac{dT}{dx}\right)_i}{\left(\frac{dT}{dx}\right)_1} = \frac{nK_1}{K_i + (n - 1) K_1} , \qquad \text{III-24}$$

where n is a constant. Substituting this equation into III-21 gives:

$$K = \frac{K_1 \left[K_2 + (n-1)K_1 - (n-1)V_2(K_1 - K_2) \right]}{K_2 + (n-1)K_1 + V_2(K_1 - K_2)} \quad . \qquad \text{III-25}$$

In equation III-25, n corresponds to 1 + X, where X is the ellipsoidal shape factor of Fricke (5)(see equation I-2). For irregularly shaped particles, there is no simple expression for the shape factor, and this semi-empirical method of separating the effects of shape from conductivity ratio seems to be appropriate. Comparing equation III-25 with III-23 shows that n is 3 for the case of spheres.

CHAPTER IV

RESULTS AND DISCUSSION

In this chapter, the correlation, as represented by equation III-25, will be compared with data from the literature and the data obtained in this investigation.

Class I Mixtures

Most of the data found in previous work fall into Class I and no additional measurements were made. For compressed metallic powders, Francl (4) could correlate his data with:

$$K = K_1(1 - V_2) , \qquad \text{I-3}$$

where K is the conductivity of the composite, K_1 is the conductivity of the pure metal, and V_2 is "void" fraction or volume fraction of air in the powder. Marathe (9) found the same behavior for compressed, powdered copper.

If the general correlation,

$$K = \frac{K_1 \left[K_2 + (n-1)K_1 - (n-1)V_2(K_1 - K_2) \right]}{K_2 + (n-1)K_1 + V_2(K_1 - K_2)} , \qquad \text{III-25}$$

holds for Class I mixtures, it should reduce to equation I-3 as a special case. For Class I mixtures, $K_1 \gg K_2$ and since n is not less than 3, $(n-1)K_1 \gg K_2$. Therefore, equation III-25 reduces to:

$$K = \frac{K_1 \left[(n-1)K_1 - (n-1) V_2 K_1 \right]}{(n-1)K_1 + V_2 K_1} ,$$
IV-1

which can be simplified to (n is 3 for this class):

$$K = K_1 \left\{ \frac{(1 - V_2)}{1 + \dfrac{V_2}{2}} \right\} .$$
IV-2

This expression is linear over any range of porosity if the change in porosity is not more than 0.2, agreeing with Marathe (9). Equation I-3 insists that the thermal conductivity be linear in V_2 with decreasing slope K_1, which does not coincide with the prediction of IV-2. However, the maximum difference between these equations occurs at 50 per cent porosity $(V_2 = 0.5)$ where they differ only by 20 per cent. Unfortunately, Francl does not present his data in a form which permits a choice between these equations. Furthermore, in order to determine experimentally which equation is more correct, the experimental precision would have to be at least 3 per cent.

On the basis of these considerations, Francl's equation (I-3) can be considered a special, simplified case of the correlation. The variability of the thermal conductivity as a function of the particle (void) shape is contained in n. Equation I-3 corresponds to a value for n of infinity. Equation IV-2 corresponds to a value for n of 3. Since only very precise measurements will distinguish between these thermal conductivities, mixtures in Class I will show scarcely any dependence on particle size or shape.

Class II Mixtures

Measurements were made on mixtures composed of aluminum particles

in rubber. Two of the mixtures contained 28 volume per cent spherical aluminum particles. In one of these, the particle diameter was 0.012 mm and in the other, 1.2 mm. These two mixtures had the same conductivity, verifying Maxwell's theoretical result for this case. Measurements were made on another mixture containing 16 volume percentage spherical aluminum particles in rubber. Figure IV-1 shows the conductivity of these three mixtures as a function of volume percentage aluminum. The curve was computed from equation III-25 with n = 3, and agrees well with the data. In these computations, a value of 118.0 $Btu/ft^2-hr-^{\circ}F/ft$. was used for the conductivity of aluminum (3).

The effect of particle shape on the conductivity of Class II mixtures was studied by measuring thermal conductivity for several mixtures, each containing 16 per cent aluminum particles which had different shapes. The measured conductivities are presented in Table IV-1, and show the shape effect. These results were used to determine n as a function of particle shape so that equation III-25 would agree with them.

The sphericity, defined as the ratio of the surface area of a sphere with a volume equal to the particle to the surface area of the particle has been used to characterize the shapes for particles falling through fluids (1). For this case, all the data for the variously shaped aluminum particles, including spheres, can be expressed by equation III-25, provided one sets n = $\frac{3}{\psi}$, where ψ is the sphericity. Figure IV-2 compares equation III-25 using this value for n. The agreement is quite satisfactory, and it is concluded that equation III-25, with a suitable choice for n, predicts the effect of particle shape. All of these mixtures were of the same composition--16 volume per cent aluminum.
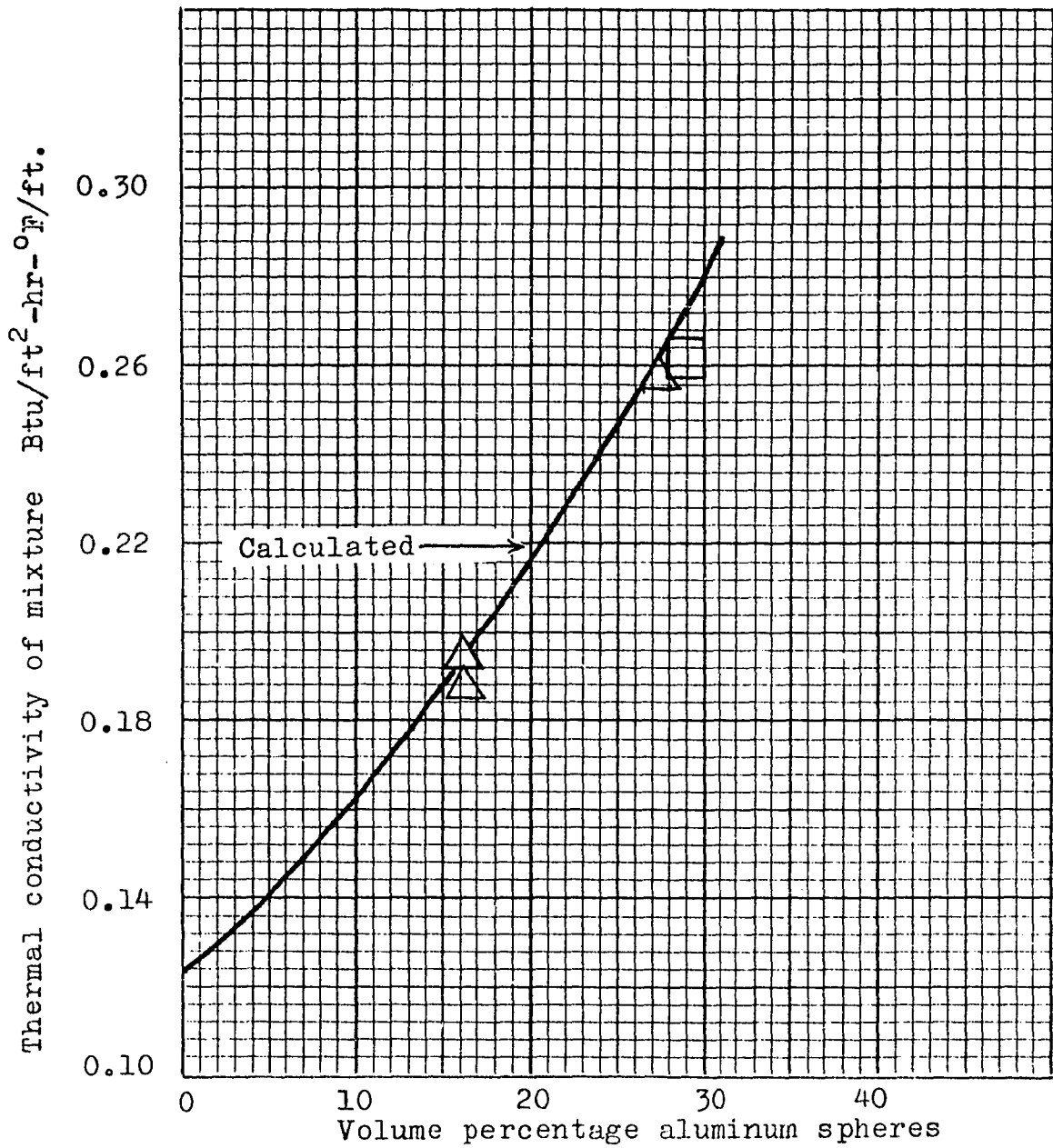
Figure IV-1. Comparison of calcul..ted and measured conductivities of mixtures of aluminum spheres in silicone 'Silastic' rubber. The curve was calculated from equation III-25 with n = 3; △ 1.2 mm diameter spheres; ☐ 0.012 mm diameter spheres
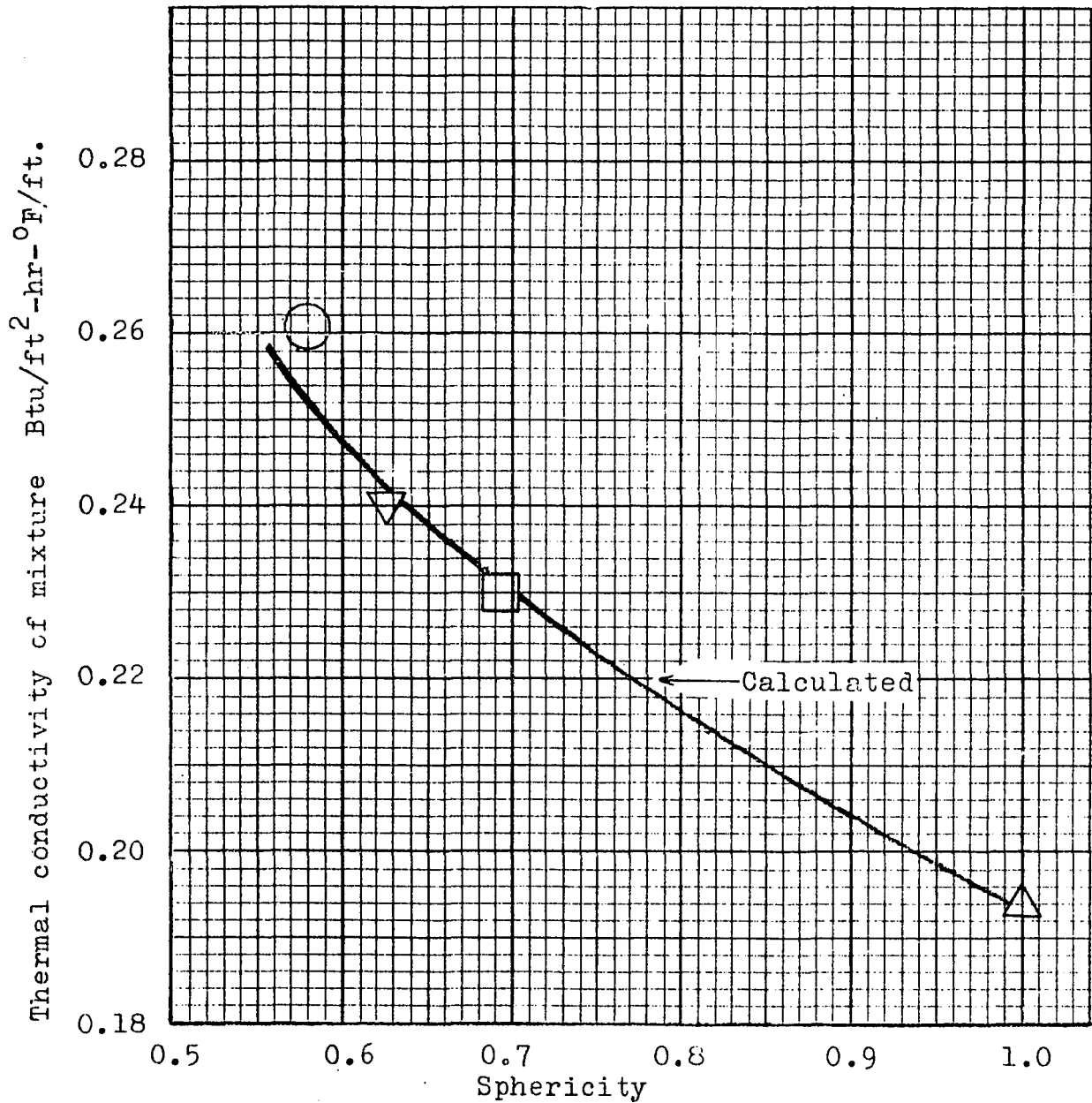
Figure IV-2. Comparison of calculated and measured conductivities of mixtures with 16 volume percentage aluminum particles of various shapes in silicone 'Silastic' rubber. The curve was calculated from equation III-25 with $n = 3/\psi$; $\triangle$ spheres; $\square$ cylinders, 5 X 1 mm diameter; $\bigcirc$ cylinders, 2.7 X 0.27 mm diameter; $\triangledown$ parallelepipeds, 1.6 X 1.6 X 0.4 mm

TABLE IV-1

MEASURED CONDUCTIVITY

Particle Shape	Particle Dimensions (mm)	Measured Conductivity Btu/ft^2-hr-$^\circ$F/ft.
Spheres	1.2 mm diameter	0.193
Cylinders	5 x 1 mm diameter	0.229
Parallelepipeds	1.6 x 1.6 x 0.4 mm	0.243
Cylinders	2.7 x 0.27 mm diameter	0.266

The correlation was tested to see if it would predict the correct composition dependence for non-spherical particles. This test was done with Johnson's (7) data on "drop-shaped" aluminum particles in gelatin. Table IV-2 shows the comparison of measured values and values computed from equation III-25 with n = 6. The comparison is satisfactory. Because n = 6 for these particles, the sphericity of these particles should be Ψ = 3/6 = 0.5. Unfortunately, Johnson did not give quantitative information about the shape of the particles, and the sphericity could not be calculated.

Class III Mixtures

Measurements were made on balsa wood particles in Silastic to determine the effect, if any, of particle size and shape in Class III mixtures. Balsa discs (Ψ = 0.5) and balsa cubes (Ψ = 0.8) were used. Table IV-3 compares the measured conductivities with those computed from equation III-25 using n = 3. In these calculations, the conductivity

TABLE IV-2

COMPARISON OF JOHNSON'S DATA WITH THE CORRELATION

Volume Per Cent Aluminum Particles	Measured Value (ref.7) Btu/ft^2-hr-$^\circ$F/ft.	Computed Value Eq. III-25 (n = 6) Btu/ft^2-hr-$^\circ$F/ft.
5.5	0.45	0.46
12.0	0.56	0.58
18.5	0.81	0.80
21.0	0.99	0.98

TABLE IV-3

COMPARISON OF EQUATION III-25 WITH DATA ON BALSA
WOOD-RUBBER MIXTURES

Volume Fraction Balsa	Sphericity of Balsa Particles	Measured Conductivity Btu/ft^2-hr-$^\circ$F/ft.	Calculated Conductivity Eq. III-25 Btu/ft^2-hr-$^\circ$F/ft.
0.25	0.5	0.098	0.093
0.25	0.5	0.097	0.093
0.25	0.8	0.095	0.093
0.14	0.5	0.108	0.107

of balsa wood was taken as 0.0242 Btu/ft^2-hr-$^\circ$F/ft. (3).

Within the accuracy of the measurements, equation III-25 agrees with these data. Also, there is no significant difference in the thermal conductivity of the two mixtures, and it can be concluded that the conductivity of Class III mixtures is not a function of particle shape.

Class IV Mixtures

Measured values of conductivity of greases were used to determine the effects of particle size and shape in this class. Measurements were made on two greases, each containing different oils and different percentages of soap. The conductivities of the two oils were also measured.

Figures IV-3 and IV-4 show microphotographs of these greases, and indicate the non-spherical shape of the soap particles. If the conductivity of such mixtures is unaffected by particle size and shape, equation III-25 should correlate these data using a value for n of 3.

In order to test the correlation, equation III-25, using n = 3, was solved for K_2, the conductivity of the discontinuous material:

$$K_2 = K_1 \left(\frac{2 + V_2 \left(\frac{\frac{K}{K_1} + 2}{\frac{K}{K_1} - 1} \right)}{V_2 \left(\frac{\frac{K}{K_1} + 2}{\frac{K}{K_1} - 1} \right) - 1} \right), \qquad \text{IV-3}$$

where K_2, K_1 and K are soap, oil and grease conductivities, respectively, and V_2 is the volume fraction soap. The soap conductivity, K_2, was calculated from the data on each grease and its oil. The two calculated values should agree if equation III-25 is valid for Class IV mix-
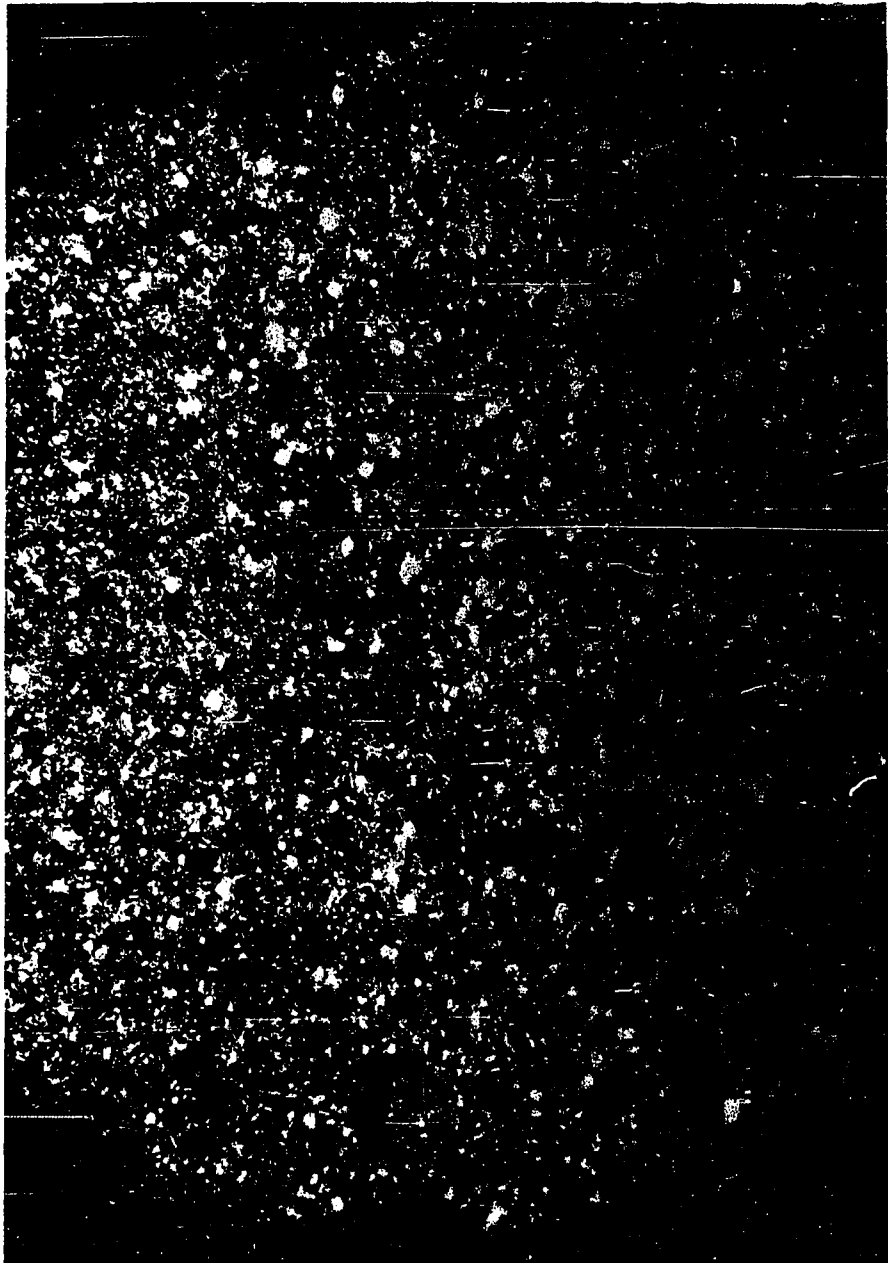
Figure IV-3. Microphotograph of grease
containing 5% soap (100 diameters)
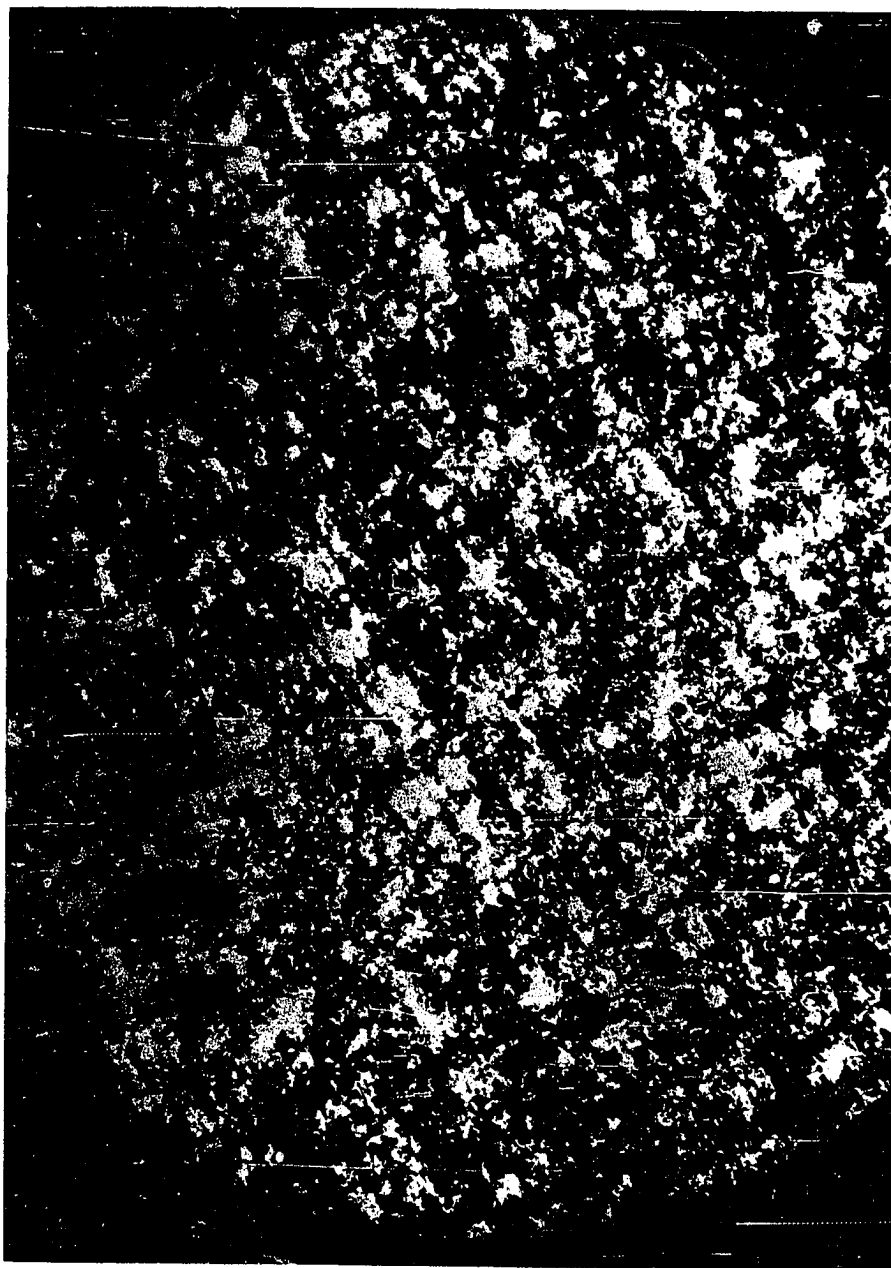
Figure IV-4. Microphotograph of grease
containing 14% soap (100 diameters)

tures. The calculated values of soap conductivity were 0.145 and 0.150 Btu/ft^2-hr-$^\circ$F/ft. at 110°F. These values are in good agreement, well within the precision of the measured grease and oil conductivities, and it is concluded that equation III-25 is valid for Class IV mixtures.

De Vries (13) and numerous other workers have pointed out an obvious conclusion which applies to both Class III and Class IV mixtures. When the conductivities of the two phases are nearly the same order, mixture conductivity changes essentially linearly with composition, and no effects of particle size and shape can be detected.

Conclusions

The thermal conductivities of widely different types of heterogeneous mixtures can be correlated with the equation:

$$K = \frac{K_1 \left[K_2 + (n-1)K_1 - (n-1)V_2(K_1 - K_2) \right]}{K_2 + (n-1)K_1 + V_2(K_1 - K_2)} ,$$

where K is the conductivity of the mixture; K_1 and K_2 are the conductivities of the continuous phase and discontinuous phase, respectively; V_2 is the volume fraction occupied by the discontinuous phase and n is an empirical constant. For mixtures in which K_2/K_1 is greater than 100, n is $3/\psi$, where ψ is the sphericity of the particles forming the discontinuous phase. For mixtures in which K_1 is approximately equal to K_2 or K_1/K_2 is greater than 100, the value of n is 3.

BIBLIOGRAPHY

1. Brown, G. G., "Unit Operations," p. 77, John Wiley, New York, 1950.

2. Dow-Corning Corporation, Midland, Michigan, Bulletin 9-399, October, 1959.

3. Forsythe, W. E., "Smithsonian Physical Tables," 9th ed., pp. 136-143, Smithsonian Institution, Washington, 1954.

4. Francl, J. and Kingery, W. D., Journal of the American Ceramic Society, 37, 99-107 (1954).

5. Fricke, H., Physical Review, 24, 575-587 (1924).

6. Grootenhuis, P., "General Discussion on Heat Transfer," pp. 363-366, American Society of Mechanical Engineers, New York, 1951.

7. Johnson, F. A., AERE R/R 2578, Atomic Energy Research Establishment, Harwell, Didcot, Berkshire, England, June, 1958.

8. Kingery, W. D. and McQuarrie, M. C., Journal of the American Ceramic Society, 37, 67-72 (1954).

9. Marathe, M. N. and Tendolkar, G. S., Transactions of the Indian Institute of Chemical Engineers, 6, 90-104 (1953).

10. Maxwell, J. C., "A Treatise on Electricity and Magnetism," Vol. 1, 3rd ed., p. 435, Dover, New York, 1954.

11. Perry, J. H., "Chemical Engineers' Handbook," 3rd ed., pp. 456-461, McGraw-Hill, New York, 1950.

12. Sibbitt, W. L., Jefferson, T. B., and Witzell, O. W., Industrial and Engineering Chemistry, 50, 1589-92 (1958).

13. Vries, D. A. de, The Thermal Conductivity of Granular Materials, Institut International du Froid, 177, Boulevard Malesherbes, Paris, France.

14. Wang, R. H., and Knudsen, J. G., Industrial and Engineering Chemistry, 50, 1667-70 (1958).

15. Woolf, J. R., and Sibbitt, W. L., Industrial and Engineering Chemistry, 46, 1947-52 (1954).

SUPPLEMENTARY BIBLIOGRAPHY

The following references can be consulted for further information.

Brophy, J. H., and Sinnott, M. J., "Thermal and Electrical Conductivity of Ductile Case Iron and Several Gray Cast Irons," Forty-first Annual Convention of American Society for Metals, Preprint No. 139 (1959).

Brown, W. F., Journal of Chemical Physics, 23, 1514 (1955).

Carslaw, H. S. and Jaeger, J. C., "Conduction of Heat in Solids," 2nd ed., pp. 425-431, Oxford, London, 1957.

Kerner, E. H., Proceedings of the Physical Society, B, 69, 802-807 (1956).

Landauer, R., Journal of Applied Physics, 23, 779-785 (1952).

Lord Rayleigh, Philosophical Magazine, 34, 481-490 (1892).

Orr, C., "Heat Transfer to Fluidized Beds," Ph. D. Dissertation, Georgia Institute of Technology, 1952.

Jeans, Sir James, "Mathematical Theory of Electricity and Magnetism," 5th ed., pp. 206-266, Cambridge University Press, 1943.

APPENDIX

DATA . 'D CALCULATIONS

TABULATED RESULTS

NOMENCLATURE

APPENDIX

This appendix contains tabulated data from which thermal conductivities were calculated. Table A-1 contains the data for Class II and Class III mixtures and Table A-2 contains the data for the greases. The properties of the materials used in the investigation are shown in Table A-3.

TABLE A-1

DATA AND RESULTS FOR CLASS II AND CLASS III

| Time and Date | Discontinuous Phase | | | | Measured Conductivity Btu/ft^2-hr-^{o}F/ft. |
	Material	Shape	Dimensions (mm)	Weight (gms)	
Cell Dimensions: I.D. = 1.5 inches, O.D. = 2.375 inches. Continuous phase contains 60 cc Silastic rubber.					
2400 5/17/60	None				0.123
0700 5/19/60	Aluminum	Spheres	1.2 dia.	60	0.263
1445 5/19/60	Aluminum	Spheres	1.2 dia.	60	0.264
2245 5/19/60	Aluminum	Spheres	1.2 dia.	30	0.195
2400 5/19/60	Aluminum	Spheres	1.2 dia.	30	0.189
2145 5/22/60	Aluminum	Spheres	0.012 dia.	62	0.268
1100 6/6/60	Aluminum	Cylinders	5 mm x 1 mm dia.	30	0.229
0200 6/8/60	Aluminum	Parallelepipeds	1.6 x 1.6 x 0.4 mm	30	0.243
2000 6/7/60	Aluminum	Cylinders	2.7 x 0.27 mm dia.	30	0.266
1800 5/27/60	Balsa	Discs	0.8 x 7.2 mm dia.	2	0.098
1800 5/29/60	Balsa	Discs	0.8 x 7.2 mm dia.	2	0.097
0100 5/30/60	Balsa	Cubes	0.8 x 0.8 x 0.8	2	0.095
2200 6/21/60	Balsa	Discs	0.8 x 7.2 mm dia.	1	0.108
Cell Dimensions: I.D. = 1.5 inches, O.D. - 3.500 inches. Continuous phase contains 450 cc Silastic rubber.					
2215 5/30/60	None				0.130

TABLE A-1--Extended

Time and Date		Heater Amperage	Thermocouple Voltage (mv)			
			Inside		Outside	
2400	5/17/60	1.41	1.468	1.468	1.248	1.248
0700	5/17/60	1.98	1.650	1.650	1.450	1.448
1445	5/19/60	1.93	1.680	1.680	1.490	1.490
2245	5/19/60	1.43	1.402	1.400	1.260	1.260
2400	5/19/60	1.51	1.404	1.404	1.260	1.260
2145	5/22/60	1.4	1.362	1.362	1.266	1.260
1100	6/6/60	0.92	1.090	1.090	1.040	1.040
0200	6/8/60	0.94	1.100	1.100	1.052	1.050
2000	6/8/60	0.93	1.164	1.164	1.120	1.120
1800	5/27/60	1.45	1.520	1.520	1.230	1.230
1800	5/29/60	1.44	1.530	1.530	1.240	1.240
0100	5/30/60	1.46	1.410	1.410	1.210	1.210
2200	6/21/60	1.4	1.550	1.550	1.300	1.300
2215	5/30/60	1.83	1.720	1.720	1.180	1.180

TABLE A-2

DATA AND RESULTS FOR GREASES

Time and Date	Thermocouple Voltage (mv)				Cold Junction Temperature °F	Middle Heater Current (amps)	Percentage Soap	Conductivity Btu/ft^2-hr-°F-ft.
	Inside		Outside					
2200 8/7/59	0.961	0.961	0.795	0.795	68	1.243	5%	0.0836
2400 8/7/59	0.964	0.970	0.800	0.802	68	1.242	5%	0.0830
1400 9/28/59	0.989	0.989	0.819	0.819	71	1.230	Oil	0.0800
0845 8/3/59	0.944	0.944	0.793	0.790	70	1.236	14%	0.0919
0300 0/25/59	0.960	0.961	0.804	0.804	70	1.220	Oil	0.0853

TABLE A-3

PROPERTIES OF MATERIALS USED

Material	Density gm/cc	Conductivity Btu/ft^2-hr-$^\circ$F/ft.
Rubber (ref. 2)	1.12	0.125
Aluminum (ref. 3)	2.70	118.
Balsa (ref. 3)	0.10	0.0242
Gelatin (ref. 7)	--	0.36

Sample Calculations Spherical Cell. Fourier's law for heat flow

across a spherical shell is:

$$Q = 4\pi K \left\{ \frac{(T_2 - T_1)}{(\frac{1}{r_2} - \frac{1}{r_1})} \right\} \quad ,$$

where Q is the heat flow; K is the conductivity; T_2 and T_1 are

outside and inside temperatures respectively; and r_2 and r_1 are the

outside and inside radii, respectively, of the shell. In terms of cur-

rent in the heater and the heater resistance:

$$Q = 3.4 R I^2 \quad ,$$

where Q is the heat flow in Btu/hr, R is the resistance in ohms, I is

the current in amperes, and 3.4 is the conversion factor from watts to

Btu/hr. Eliminating Q from these two equations and solving for K

gives:

$$K = \frac{3.4 \left(\frac{r_1 - r_2}{r_1 r_2} \right) 12 R I^2}{4\pi(T_2 - T_1)} \quad ,$$

where r_1 and r_2 are in inches. For copper-constantan thermocouples

at the temperature of the measurements:

$$T_2 - T_1 = \frac{\mathcal{E}_2 - \mathcal{E}_1}{23} \quad ,$$

where $\mathcal{E}_2$ and $\mathcal{E}_1$ are the outside and inside thermocouple voltages,

respectively. Eliminating $(T_2 - T_1)$ gives:

$$K = \frac{3.4(12)23 \left(\frac{r_1 - r_2}{r_1 r_2} \right) R I^2}{4\pi(\mathcal{E}_2 - \mathcal{E}_1)} \quad .$$

The heater resistance was 0.4 ohms. For the small cell $r_2 = 1.188$; for

the large cell $r_2 = 1.75$ and $r_1 = 0.75$ for both cells. Using these values gives:

$$K = 13.5 \left(\frac{I^2}{\varepsilon_1 - \varepsilon_2} \right)$$

for the small cell and

$$K = 20.9 \left(\frac{I^2}{\varepsilon_1 - \varepsilon_2} \right)$$

for the large cell. With these equations, K could be calculated from the current in the heater and the voltages of the inside and outside thermocouples.

Concentric Cylinder Cell. For this cell the conductivity is given by:

$$K = \frac{12 \left(\ln \frac{r_2}{r_1} \right) Q}{-2 \pi L (T_2 - T_1)} \quad ,$$

where Q is the heat flow in Btu/hour; r_2 and r_1 are outside and inside radii, respectively, of the annulus; T_2 and T_1 are the outside and inside temperatures and L is the length of the center section. For this cell:

$$L = 7.26 \text{ inches,}$$

$$\ln \frac{r_2}{r_1} = 0.0962 \quad ,$$

$$Q = 3.41 \, R \, I^2 = 15.05 \, I^2 \quad ,$$

$$T_2 - T_1 = \frac{\varepsilon_2 - \varepsilon_1}{23} \quad .$$

Using these values gives:

$$K = 8.33 \left(\frac{I^2}{\varepsilon_1 - \varepsilon_2} \right) \quad ,$$

where I is the current in the middle heater and $\mathcal{E}_1 - \mathcal{E}_2$ is the voltage difference between the inside and outside thermocouples. This calculation can be illustrated with the data of 0300, 0/25/59.

$$\mathcal{E}_1 = 0.961 ,$$

$$\mathcal{E}_2 = 0.804 ,$$

$$I = 1.220 ,$$

$$I^2 = 1.4884 .$$

Putting these values into the equation:

$$K = 8.83 \frac{I^2}{\mathcal{E}_1 - \mathcal{E}_2} ,$$

gives K = 0.085.

In designing the concentric cylinder cell, it was assumed that when a reading was being made there would be no temperature difference across the Teflon plugs which separated the guard heaters from the middle heater. There was usually about 0.1 to 0.5°F difference, however, and this effect had to be estimated to see if it would affect the measured values of conductivity. The heat flow across one plug is calculated as follows:

$$\text{area of Teflon plug} = \frac{\pi}{4} (1.5)^2 \frac{1}{144} = 0.012 \text{ ft}^2 ,$$

$$\text{conductivity of Teflon} = 0.1 \text{ Btu/ft}^2\text{-hr-}°\text{F/ft. },$$

$$\text{length for heat flow} = 0.031 \text{ ft. },$$

$$\Delta T = 0.5 ,$$

$$Q = \frac{(0.1)(.012)(0.5)}{.031}$$

$$= 0.002 \text{ Btu/hr.}$$

Also, heat will flow down the lead wires:

> 5   30 gage Copper wires ,
>
> 5   30 gage Constantan wires ,
>
> 4   24 gage Copper wires .

Total area of wire = $2 \ (10)^{-4} \ ft^2$.

> $K = 200$,
>
> $L = 0.031$,
>
> $\Delta T = 0.5$,
>
> $Q = 0.053$ Btu/hr.

Total heat lost $= 2(0.053 + 0.002) = 0.110$ Btu/hr.

Total heat dissipated in middle heater $= 15$ Btu. Thus the heat loss is about 0.7 per cent of the heat dissipated in the middle heater and this loss was neglected.

NOMENCLATURE

K   thermal conductivity of the mixture--Btu/ft^2-hr-$^oF/ft$.

K_1 thermal conductivity of the continuous phase.

K_2 thermal conductivity of discontinuous phase.

V_2 volume fraction of discontinuous phase-dimensionless.

X   "shape factor" for ellipsoids in Fricke's equation--dimensionless.

n   empirical shape factor--dimensionless.

ψ sphericity--dimensionless.

T   temperature--^oF.

Q   heat flow--Btu/hr.

A   area--ft^2.